



**HAL**  
open science

**Innovative combination of tracing methods to differentiate between legacy and contemporary PAH sources in the atmosphere-soil-river continuum in an urban catchment (Orge River, France)**

Claire Froger, Sophie Ayrault, Johnny Gasperi, Emilie Caupos, Gaël Monvoisin, O. Evrard, Cécile Quantin

► **To cite this version:**

Claire Froger, Sophie Ayrault, Johnny Gasperi, Emilie Caupos, Gaël Monvoisin, et al.. Innovative combination of tracing methods to differentiate between legacy and contemporary PAH sources in the atmosphere-soil-river continuum in an urban catchment (Orge River, France). *Science of the Total Environment*, 2019, pp.448-458. 10.1016/j.scitotenv.2019.03.150 . hal-02067746

**HAL Id: hal-02067746**

**<https://enpc.hal.science/hal-02067746>**

Submitted on 7 Jul 2020

**HAL** is a multi-disciplinary open access archive for the deposit and dissemination of scientific research documents, whether they are published or not. The documents may come from teaching and research institutions in France or abroad, or from public or private research centers.

L'archive ouverte pluridisciplinaire **HAL**, est destinée au dépôt et à la diffusion de documents scientifiques de niveau recherche, publiés ou non, émanant des établissements d'enseignement et de recherche français ou étrangers, des laboratoires publics ou privés.

1 **Innovative combination of tracing**  
2 **methods to differentiate between**  
3 **legacy and contemporary PAH**  
4 **sources in the atmosphere-soil-river**  
5 **continuum in an urban catchment**  
6 **(Orge River, France)**

7  
8 Claire Froger<sup>\*,1,2</sup>, Sophie Ayrault<sup>1</sup>, Johnny Gasperi<sup>3</sup>, Emilie Caupos<sup>3</sup>, Gaël Monvoisin<sup>2</sup>,  
9 Olivier Evrard<sup>1</sup>, Cécile Quantin<sup>2</sup>

10  
11 \*Corresponding author: c

12 laire.froger@lsce.ipsl.fr

13 Phone: +33 169824357

14 Address: Bat. 714, CEA – Orme les Merisiers, 91198, Gif-sur-Yvette, France

15  
16 <sup>1</sup> Laboratoire des Sciences du Climat et de l'Environnement (LSCE/IPSL), CEA-CNRS-  
17 UVSQ, Université Paris-Saclay, 91198 Gif-sur-Yvette, France

18 <sup>2</sup> Géosciences Paris Sud (GEOPS), Université Paris-Sud – CNRS- Université Paris-Saclay,  
19 91400 Orsay, France

20 <sup>3</sup> Laboratoire Eau Environnement et Systèmes Urbains (LEESU), Université Paris-Est Créteil,  
21 UMR MA 102- Agro ParisTech, 94010 Créteil, France

22  
23  
24 Abstract

25 Polycyclic aromatic hydrocarbons (PAH) have been released by human activities during more  
26 than a century, contaminating the entire atmosphere – soil – river continuum. Due to their  
27 ubiquity in the environment and their potential severe biological impacts, PAH became  
28 priority pollutants and were targeted by environmental public agencies. To better manage  
29 PAH pollution, it is necessary to identify unambiguously the sources and pathways of those  
30 compounds at the catchment scale, and to evaluate the persistence of historical PAH pollution  
31 in the environment especially in those urban contexts concentrating multiple PAH sources.  
32 Accordingly, the current research monitored the contamination in atmospheric fallout, soils  
33 and rivers of a 950-km<sup>2</sup> catchment (Orge River) characterized by an increasing urban gradient  
34 in downstream direction, and located in the Seine River basin characterized by a high level of  
35 PAH legacy contamination. A combination of various approaches was used, including the  
36 widely used PAH diagnostic ratios, together with innovative methods such as PAH  
37 correlations and sediment fingerprinting using fallout radionuclides to clearly identify both  
38 the origin of PAH and their main PAH pathways to the river. The results demonstrated the  
39 persistence of legacy PAH contamination in the catchment, responsible for the signature of  
40 the suspended particulate matter currently transiting in the Orge River. They underlined the  
41 conservation of PAH through the soil – river continuum. Finally, urban runoff was  
42 demonstrated to provide the main PAH source to the river in the densely urbanized area by  
43 both PAH correlations and sediment fingerprinting. These results were used to model PAH  
44 concentrations in those particles supplied from urban areas to the river.

45 Keywords: PAH ratios, urban runoff, legacy contamination, sediment fingerprinting

46

## 47 1. Introduction

48 Human activities have led to deleterious impacts on aquatic ecosystems as a result of the  
49 discharge of numerous contaminants into the environment. Among these harmful substances,

50 polycyclic aromatic hydrocarbons (PAHs) released by the incomplete combustion or the  
51 pyrolysis of organic matter have been listed as priority pollutants by environmental state  
52 agencies since the 1970s due to their adverse effects on health (Grimmer, 1985). Accordingly,  
53 policies and regulations have been implemented to improve the river quality and to control  
54 further contaminant releases. In Europe, the Water Framework Directive (WFD, Directive  
55 2000/60/EC) fixes the target concentrations for multiple contaminants in water bodies, in  
56 order to improve their chemical quality. In France, numerous river basins including the Seine  
57 River basin exceed the target concentrations with values reaching up to  $20 \text{ mg.kg}^{-1}$  in the  
58 particulate fraction (Fernandes et al., 1997), threatening the achievement of the good chemical  
59 status. Accordingly, the identification of those sources supplying PAH contamination to rivers  
60 is required to improve the current management of water bodies. As PAH contamination is  
61 widespread in Western Europe because of the continuous atmospheric releases of these  
62 substances since 1850 (Fernández et al., 2000), it is particularly important to determine  
63 whether the high levels of contamination observed nowadays in rivers are mainly explained  
64 by the remobilization of legacy pollution or by the current releases of these substances.

65 Several tracing approaches have been developed during the last several decades to identify the  
66 main sources of PAH in the environment (Budzinski et al., 1997; Gateuille et al., 2014b;  
67 Yunker et al., 2002). The most frequent technique corresponds to the calculation of diagnostic  
68 molecular ratios. This approach is based on the use and combination of ratios between  
69 different PAH, as the contribution of specific molecules is characteristic of a given source  
70 type, typically the combustion of either biomass (coal, wood, grass), or that of crude oil and  
71 fossil fuel (Ravindra et al., 2008). The combination of two ratios is generally used to  
72 discriminate PAH according to their pyrogenic, petrogenic or mixed origin (Kavouras et al.,  
73 2001; Tobiszewski and Namieśnik, 2012). However, several studies pointed out the  
74 sensitivity of those ratios to environmental processes such as oxidation and photo-oxidation

75 leading to the preferential degradation of some PAH, therefore modifying the related ratios  
76 (Biache et al., 2014; Zhang et al., 2005). Moreover, as these ratios are not specific to a  
77 particular source, their interpretation remains limited and insufficient in complex urban  
78 catchments where the identification of well-localized sources is required. Other approaches  
79 involve statistical analyses such as principal component analysis (PCA), hierarchical cluster  
80 analysis (HCA) or modelling techniques like the positive matrix factorization (PMF) to  
81 identify sources (Motelay-Massei et al., 2003; Sofowote et al., 2011; Xu et al., 2016). Those  
82 statistical analyses take into account all the PAH molecules measured when processing the  
83 datasets, with the particularity for PCA and HCA to cluster PAH molecules or samples  
84 sharing similar characteristics. The PMF models are more complex and their results provide  
85 theoretical PAH profiles of the sources with their respective contribution, which can then be  
86 compared to the potential sources of PAH. Although statistical approaches may be powerful,  
87 caution must be taken when interpreting their outputs, as they strongly depend on data quality  
88 and quantity, and do not consider the multiple processes that may affect the fate of PAH in the  
89 environment (biodegradation, oxidation...). Finally, nitro and oxy-PAHs, which are  
90 commonly investigated because of their mutagenicity (Umbuzeiro et al., 2008), appeared to  
91 provide powerful tracers of some anthropogenic sources such as diesel combustion (Anyanwu  
92 and Semple, 2015; Keyte et al., 2016). However, their measurement requires further analytical  
93 developments, currently limiting their widespread use as diagnostic tracers.

94 In addition, the identification of PAH sources is challenging as their contribution may vary  
95 throughout time (Garban et al., 2002; Harrison et al., 1996). The impact of multiple local  
96 sources (household heating, vehicular emissions, industrial emissions), combined with long-  
97 range emissions or the remobilization of legacy pollution could complicate the identification  
98 of those sources (Haugland et al., 2008; Schiffman and Boving, 2015). As a consequence, few  
99 studies have investigated the pathways of PAH in the atmosphere – soil – river continuum

100 (Gateuille et al., 2014a; Gocht et al., 2007; A. Motelay-Massei et al., 2007). The objective of  
101 the current research was to identify the PAH sources and pathways in an urban catchment and  
102 to differentiate between legacy and current PAH sources, through the investigation of PAH  
103 contamination in the atmosphere, the soil and the river during a hydrological year. To achieve  
104 this goal, the Orge River catchment was selected as it is representative of urbanized  
105 catchments (Froger et al., 2018) and located in an early industrialized region. Source  
106 identification using PAH diagnostic ratios was combined with new approaches such as PAH  
107 correlations and the measurement of fallout radionuclides used for sediment fingerprinting to  
108 better discriminate both sources and pathways of particle-bound PAH in the atmosphere, the  
109 soils and the river.

110

## 111 2. Material and methods

### 112 2.1. Study site

113 All river water, atmospheric and road sediments samples were collected in the Orge River  
114 catchment, which is located 30 km south of Paris City and drains into the Seine River (Figure  
115 1; see Froger et al., 2018). Four sampling sites were selected based on their urbanization rate  
116 and previous work on the catchment (Le Pape et al., 2012): three were located on the main  
117 stem of the Orge River, whereas a fourth site was located on its main tributary, the Yvette  
118 River. The proportion of urban areas strongly increases in downstream direction, varying  
119 from 1% in upper catchment parts to 56% at the outlet. This change is reflected by the  
120 evolution of the population densities in the drainage areas (from 300 inhabitants per km<sup>-2</sup> at  
121 the most rural study site – Dourdan (“D”), to 5,000 inh.km<sup>-2</sup> at Viry (“V”, nearby the outlet).  
122 The geology of the catchment is characterized by Eocene formations including carbonate  
123 rocks, marls and gypsum, and Oligocene formations dominated by Fontainebleau sands (Le  
124 Pape et al., 2012).

125 In addition to river water and sediment samples, four road deposited sediments (RDS) were  
126 collected at the most urbanized site in Viry, nearby the local river sampling site, and samples  
127 of atmospheric fallout were collected on the roof of a building at Orsay.

128

## 129 2.2. Hydrological conditions

130 River water sampling was conducted during a hydrological year with the organization of five  
131 campaigns from January to December 2016. Daily water discharge at the outlet varied  
132 throughout the year from 1.6 to 39.5 m<sup>3</sup>.s<sup>-1</sup> with a mean value of 3.5 m<sup>3</sup>.s<sup>-1</sup>. The sampling  
133 campaigns were organized to be representative of those hydrological conditions observed  
134 throughout the year in the Orge River (Figure 2). Accordingly, one campaign was organized  
135 during the low flow period (< 2 m<sup>3</sup>.s<sup>-1</sup> at the outlet, August 2016), three campaigns occurred  
136 when the water flow was comprised between 2 and 5 m<sup>3</sup>.s<sup>-1</sup> (January, November and  
137 December 2016) and one campaign was conducted during a flood (water flow exceeding 5  
138 m<sup>3</sup>.s<sup>-1</sup>; April 2016). Sampling was also conducted during the extreme flood of June 2016 with  
139 a peak discharge of 39.5 m<sup>3</sup>.s<sup>-1</sup> recorded at the outlet.

140

## 141 2.3. Sampling and PAH analysis

### 142 2.3.1. River, atmospheric deposition and road deposited sediment sampling

143 Punctual samples of river water (n = 32) were collected in the middle section of the river at 20  
144 – 30 cm depth using 2-L brown glass bottles preliminary washed with detergent (TFD4) and  
145 grilled at 500°C (Bressy et al., 2012). The extraction protocol was rapidly conducted on the  
146 samples on the same day as the sampling. In addition, sediment traps composed of metal  
147 bottles submerged in the river (20 – 30 cm depth) were deployed during 4 to 5 days to collect  
148 suspended particulate matter (SPM) by sedimentation for a longer period (n = 22). Suspended

149 particulate matter recovered from the traps were decanted, the supernatant was removed and  
150 the suspended solid was freeze-dried (Gateuille et al., 2014a). After the flood of June 2016,  
151 floodplain sediments were collected overbank in Dourdan, Egly, Yvette and Viry after the  
152 flood recession.

153 Samples of total atmospheric deposition were collected in Orsay, near the Yvette River  
154 monitoring site, from the February 1<sup>st</sup>, 2016 to March 30, 2017 (Figure 1). Two funnels with  
155 21 and 28 cm diameters were installed and connected to brown glass bottle collectors.  
156 Atmospheric fallout samples (n = 26) were collected after variable periods, the median  
157 duration between successive sample collections was 16 days.

158 Finally, four RDS were sampled on the road bordering the river sampling site at Viry. The  
159 samples were freeze-dried and sieved to 200  $\mu\text{m}$  as PAH are considered to be mainly  
160 associated with the fine particle fraction (Pratt and Lottermoser, 2007) and the size of  
161 particles washed during runoff is mainly under 300  $\mu\text{m}$  (El-Mufleh et al., 2011; Revitt et al.,  
162 2014; Roger et al., 1998).

163

#### 164 2.3.2. Sample preparation

165 The analytical protocol has been detailed in previous studies (Bressy et al., 2012; Froger et al.,  
166 2019; Lorgeoux et al., 2016). In brief, instantaneous samples of river water and atmospheric  
167 fallout were filtered just after sampling, first on quartz filters GF/D (porosity of 2.7  $\mu\text{m}$ ) then  
168 on GF/F (porosity 0.47  $\mu\text{m}$ ) preliminarily grilled at 500°C. Filters were then freeze-dried.  
169 Following filtration, extraction was done on a solid phase siliceous cartridge C18 (6 mL and  
170 2000 mg). Solid sample extraction (atmospheric particles, river SPM and RDS) was  
171 performed using a microwave assisted extraction (Microwave 3000, Anton Paar). Samples  
172 were introduced in close bottles with a mixture of dichloromethane and methanol, heated at



173 100°C during 10 minutes (Lorgeoux et al., 2016). A sample of a certified material (i.e. a lake  
174 sediment standard, NIST 1944) was also extracted in the same sequence to validate the  
175 analytical method. To avoid interferences during the analysis, the purifications of all extracted  
176 samples were performed using silica gel columns (2.1 g of silica gel) to separate the different  
177 compound families using various solvent mixtures. Before extraction, an internal standard  
178 containing 6 deuterated PAH (naphthalene-D8, acenaphtheneD10, phenanthreneD10,  
179 pyreneD12, chryseneD12 and peryleneD12) was added to each sample, for both dissolved and  
180 particulate fractions.

181

### 182 2.3.3. PAH analysis

183 PAH concentrations in the dissolved and particulate phases (i.e. SPM) of river water samples  
184 and atmospheric fallout, and in the road deposited sediments were measured by gas  
185 chromatography coupled with a mass spectrometer (GC-MS, column RTX5SIL-MS (Restek,  
186 60 m, 0.25 mm ID, 0.25 µm df)) used in SIM mode. Helium was the vector gas and the  
187 injection volume was 1 µL, the samples were heated at 330°C for 6 minutes before  
188 measurement. PAH were quantified using internal standards. The following PAH were  
189 measured: fluorene (Fl), phenanthrene (Phe), anthracene (Ant), fluoranthene (Flh), pyrene  
190 (Py), benzo(a)anthracene (BaA), chrysene (Chry), benzo(b)fluoranthene (BbF),  
191 benzo(k)fluoranthene (BkF), benzo(a)pyrene (BaP), indeno(1,2,3-cd)pyrene (IndP),  
192 dibenzo(a,h)anthracene (DbahA) and benzo(g,h,i)perylene (BghiP). The results were  
193 expressed as the sum of 13PAHs ( $\Sigma$ 13PAHs). QA and QC were detailed in the supplementary  
194 material of Froger et al. (2019). Results found for naphthalene, acenaphtylene and  
195 acenaphtene were not considered in the current research, as these compounds are too volatile  
196 to be correctly quantified with the protocol used in this study.

197

198 2.3.4. Modeling the PAH profile of urban particles

199 Fallout radionuclide concentrations measured in the Orge River SPM were reported in a  
200 previous paper (Froger et al., 2018) and showed a linear increase in  $^7\text{Be}$  and  $^{210}\text{Pb}_{xs}$  activities  
201 in SPM collected in downstream direction (Fig. S2). This finding was interpreted as reflecting  
202 the increasing supply of recently eroded particles supplied by urban areas to the river through  
203 urban runoff (RDS source; see Froger et al., 2018 for hypothesis development). Moreover, the  
204 linear trend suggested that agricultural soils depleted in both  $^7\text{Be}$  and  $^{210}\text{Pb}_{xs}$  provided the  
205 main source of particles transiting the river in upper catchment parts. Based on these results, a  
206 two end-member equation (Eqs. 1 and 2) was established to estimate the respective  
207 proportions of particles supplied by agricultural land ( $P_{AP}$ , in %) and those delivered by urban  
208 areas ( $P_{UP}$ , in %) to those SPM transiting the Orge River at each monitoring site.

209 
$$^7\text{Be}_{SPM} = P_{AP} ^7\text{Be}_{old\ particles} + P_{UP} ^7\text{Be}_{recent\ particles} \quad \text{Eq. 1}$$

210 
$$^{210}\text{Pb}_{xs\ SPM} = P_{AP} ^{210}\text{Pb}_{xs\ old\ particles} + P_{UP} ^{210}\text{Pb}_{xs\ recent\ particles} \quad \text{Eq. 2}$$

211 These proportions were applied to PAH concentrations to estimate the PAH concentrations of  
212 the recent particles, which will be referred to as theoretical urban particles (TUP) ( $\text{PAH}_{TUP}$ ).  
213 In this model, PAH conservation was assumed during their transfer from the source to the  
214 sampling site. All the calculations were conducted using the solver module of the Excel  
215 software to find the solution to an equation system with multiple conditions, involving an  
216 iterative process to converge to the most accurate result. To calculate the final PAH  
217 concentrations of theoretical urban particles, each SPM sample  $j$  was modelled to correspond  
218 to a mixture of agricultural particles and TUP ( $\text{MPAH}_{SPM,i,j}$ ) (Eq. 3).

219 
$$[\text{MPAH}]_{SPM,i,j} = (P_{AP,j}[\text{PAH}]_{i,AP} + P_{UP,j}[\text{PAH}]_{i,j\ TUP}) \quad \text{Eq. 3}$$

220 
$$e_j = \sum_{i=1}^{13} \frac{[MPAH]_{SPM,i,j} - [PAH]_{SPM,i,j}}{[PAH]_{SPM,i,j}} \quad \text{Eq. 4}$$

221 With  $MPAH_{SPM,i,j}$  the modeled concentration of the PAH molecule  $i$  in the SPM sample  $j$ ;  $P_{AP,j}$   
 222 and  $P_{UP,j}$  the proportions (in %) of particles originating from agricultural soils and from urban  
 223 areas in the SPM sample  $j$  calculated based on the fallout radionuclide results;  $[PAH]_{i,AP}$  the  
 224 concentration of the PAH molecule  $i$  in particles originating from agricultural soils reported  
 225 by Gasperi et al., (2016);  $[PAH]_{i,j,TUP}$  the modeled concentration of the PAH molecule  $i$  in  
 226 theoretical urban particles contained in the SPM sample  $j$ , which is the unknown value that  
 227 will be estimated. This estimation is thus the result of iterations minimizing  $e$  (Eq. 4), the sum  
 228 of the differences between the modeled PAH concentrations in SPM ( $MPAH_{SPM,i,j}$ ) and the  
 229 measured PAH concentrations ( $PAH_{SPM,i,j}$ ).

230 The final PAH concentrations profile (Eq. 5) and the associated standard errors in the  
 231 theoretical urban particles were calculated as the mean value of the  $[PAH]_{i,j,TUP}$  estimated  
 232 from each SPM sample  $j$ .

233 
$$[PAH]_{i,TUP} = \sum_{j=1}^n \frac{[PAH]_{i,j,TUP}}{n} \quad \text{Eq. 5}$$

234

### 235 3. Results and discussion

#### 236 3.1. PAH contamination levels and variations in sediment

237 The concentrations of PAH in the atmospheric fallout and river SPM have been detailed in  
 238 Froger et al., (2019). No temporal tendency in PAH variations was observed in atmospheric  
 239 fallout particles, characterized by  $\sum 13PAH$  concentrations varying from 5 to 93  $\mu\text{g.g}^{-1}$ . On the  
 240 contrary, SPM contamination of the Orge River ranged from 1.1 to 45.2  $\mu\text{g.g}^{-1}$  ( $\sum 13PAH$ )  
 241 with an increase in PAH concentrations when moving in downstream direction, from a  
 242 median value of 3.3  $\mu\text{g.g}^{-1}$  in Dourdan to 8.5  $\mu\text{g.g}^{-1}$  in Viry ( $\sum 13PAH$ ). In addition, the

243 proportions of 4 rings and 5-6 rings PAH amounted to respectively 43% and 44% of the total  
244 PAH content, with only 11% of the total provided by the 3 rings PAH. Similar increasing  
245 trends in downstream direction were observed for all compounds (Kruskal-Wallis test,  
246  $p < 0.05$ ) although the lowest *p-value* (i.e. 0.0002) was obtained for 4 PAHs indicating their  
247 larger spatial variability. The concentrations of 4 rings PAH increased from 1.1 to 3.9  $\mu\text{g}\cdot\text{g}^{-1}$   
248 (median concentrations) from Dourdan to Viry, those of 5-6 rings PAH raised from 1.3 to 3.6  
249  $\mu\text{g}\cdot\text{g}^{-1}$  whereas the increase was more limited for 3 rings PAH concentrations (from 0.4 to 0.8  
250  $\mu\text{g}\cdot\text{g}^{-1}$ ; Fig. S1).

251 Moreover, PAH concentrations in road deposited sediments ranged from 5.6 to 15.6  $\mu\text{g}\cdot\text{g}^{-1}$   
252 ( $\Sigma 13\text{PAH}$ ) with respective proportions of 4 (45 %) and 5-6 rings (41%) PAH similar to those  
253 found in river SPM. The PAH contents in RDS were similar to those measured in road  
254 sediments studied by Brown and Peake (2006), although in the lower range of others studies  
255 (Aryal et al., 2005; Murakami et al., 2005)

### 256 3.2. Tracing sources using Molecular Ratios

257 The four most frequently used molecular diagnostic ratios, i.e. Flh/(Flh + Py), BaA/(BaA +  
258 Chry), IndP/(IndP + BghiP) and Phe/(Phe + Ant) (e.g. Ravindra et al., 2008), were  
259 investigated in this study (Figure 3). Signatures of particulate samples from the Orge  
260 catchment, SPM, atmospheric particles, RDS and flood sediments, were compared (Figure 3).  
261 As molecular diagnostic ratios found in the Orge River SPM did not vary in downstream  
262 direction (see Table S2), they were considered as a single group despite their collection at 4  
263 different sites. Those PAH ratios from the Orge catchment were compared with the PAH  
264 signatures derived from the compilation of literature data (Table 1), including potential  
265 sources of particulate-bound PAH corresponding to soil samples (Gaspéri et al., 2018) and  
266 runoff particles collected in the densely urbanized catchment of Sucy (south-east of Paris)  
267 (Gaspero et al., 2018 (Report)). The latter were selected as Sucy catchment presents similar

268 characteristics to those found at Viry site, in terms of drainage surface and urbanization rate.  
269 The signature of legacy PAH contamination was also reconstructed based on the analysis of  
270 successive layers from a sediment core collected in the alluvial plain of the Seine River  
271 (Lorgeoux et al., 2016), which recorded PAH concentrations from the early 1950s to 2004.  
272 Evolution of PAH concentrations showed a drastic increase from 1950 to 1963 before a  
273 decrease between 1963 and 1970 and then a stabilization after 1970. Accordingly, those  
274 values were divided into two periods: '1950 – 1963' and '1970 – 2004'.

275

276 The combination of  $\text{Ind}/(\text{IndP} + \text{BghiP})$  with  $\text{Flh}/(\text{Flh} + \text{Py})$  ratios (Figure 3a) indicated a  
277 PAH origin at the boundary between fossil fuel and coal/wood combustion for all particulate  
278 samples, except for soils. The molecular ratio of  $\text{IndP}/(\text{IndP} + \text{BghiP})$  (Figure 3a) remained  
279 very stable and similar in atmospheric particles, SPM, RDS, Seine River sediments and runoff  
280 particles. These constant signatures in very different sample types is supported by Schwientek  
281 et al., (2013) study demonstrating similar PAH patterns in river SPM throughout the  
282 catchments. In addition, the results of previous studies showing the stability of PAH with a  
283 high molecular weight (HMW) in various environmental conditions compared to that of  
284 lighter PAH corroborate the conclusion of the current study (Biache et al., 2014; Zhang et al.,  
285 2005). In contrast, soil samples showed very heterogeneous signatures, which were not related  
286 to changes in spatial location or land use. This scattered pattern of values found in soils for  
287 this ratio could be explained by the low concentrations, close to the detection limits, of IndP  
288 and BghiP found in these samples, resulting in the higher variability of the ratio. Compared to  
289  $\text{Ind}/(\text{IndP} + \text{BghiP})$ , the  $\text{Flh}/(\text{Flh} + \text{Py})$  ratio showed the occurrence of differences between the  
290 signature of atmospheric particles and that of SPM suggesting a stronger contribution of fossil  
291 fuel combustion in atmospheric particles than in SPM. The large range of values found in the  
292 signatures of the Orge SPM, with  $\text{Flh}/(\text{Flh} + \text{Py})$  ratios varying from 0.4 to 0.8 was likely

293 related to the sampling period (Kruskal Wallis test,  $p < 0.05$ ), as the highest ratios were found  
294 in the samples collected in November 2016 (median value of 0.62 for all sites), whereas the  
295 lowest values were found in January 2016 (median value of 0.52). The reason for these  
296 temporal variations could not be determined as both campaigns were characterized by similar  
297 hydrological and meteorological conditions.

298 When combining the  $BaA/(BaA + Chry)$  and the  $Flh/(Flh + Py)$  ratios (Fig. 3b), two trends  
299 could be highlighted: the first one includes atmospheric particles together with RDS and part  
300 of the runoff particles, while the second trend integrates Orge SPM and flood sediments, soil  
301 samples, and Seine River sediments. Diagnostic ratios indicated that PAH from the first group  
302 originated from the fossil fuel combustion, whereas the second group signatures reflected the  
303 occurrence of mixed sources and biomass combustion. This could be due to point-based  
304 sources of fossil fuel combustion for atmospheric and road particles (Ravindra et al., 2006),  
305 whereas river sediments may cumulate PAH inputs from multiple sources. Finally, the  
306 temporal variations observed for the  $Flh/(Flh + Py)$  ratio of SPM were not found for the  
307  $BaA/(BaA + Chry)$  ratio.

308 The combination of  $Phe/(Ant + Phe)$  with  $Flh/(Flh + Py)$  ratios, however, underlined a  
309 different pattern (Fig. 3c), and most samples (including Orge SPM, RDS, atmospheric  
310 particles and soil samples) were shown to match the signatures of crude oil and fossil fuel  
311 combustion. Nevertheless, the  $Phe/(Ant + Phe)$  ratio was shown to be the most sensitive to  
312 environmental processes such as biodegradation and abiotic oxidation inducing the  
313 occurrence of significant modifications of source signatures (Alam et al., 2013; Katsoyiannis  
314 and Breivik, 2014). The observed petrogenic signature may therefore be attributed to the  
315 preferential degradation of anthracene, particularly sensitive to oxidation, which resulted in  
316 increased ratio values (Biache et al., 2014; Zhang et al., 2005).

317 Among the explored molecular ratios, the combination of Flh/(Flh + Py) and BaA/(BaA +  
318 Chry) (Fig. 3b) provided the most explicit insights into the sources of PAH in the Orge River  
319 catchment. On the one hand, PAH found in atmospheric particles and RDS were mainly  
320 supplied by the fossil fuel combustion, and their signatures matched those of runoff particles.  
321 On the other hand, PAH found in the Orge SPM reflected a fossil fuel and biomass  
322 combustion origin, and showed PAH signatures similar to those of soil samples and Seine  
323 River sediments. Nevertheless, the contradictions in sources identified by the PAH ratios  
324 underlined the caution needed when using these approaches to define PAH sources.  
325 Moreover, molecular diagnostic ratios did not reflect the increase in PAH concentrations  
326 observed in the Orge SPM from up to downstream sites and therefore provided no additional  
327 insight into the source of PAH inputs originating from those urban areas located downstream.

328

### 329 3.3. PAH correlation

330 Correlations between PAH have been used in several studies as a complement to PAH ratios  
331 for conducting PAHs source identification (Bertrand et al., 2015; Soclo et al., 2000). In the  
332 current research, SPM PAH concentrations for several 4 to 6 rings PAH showed a significant  
333 correlation with a coefficient above 0.9 (Table S1). For instance, Chry, Flt and BaA displayed  
334 correlation coefficients comprised between 0.90 and 0.97. Higher molecular weight PAH with  
335 5 and 6 rings (BaP, IndP, DbahA, BghiP) also showed high intercorrelation with coefficients  
336 from 0.93 to 0.99. Interestingly, 4 rings PAHs appeared to better represent PAH inputs from  
337 urban areas in the lower section of the Orge River as shown by the increase of PAH  
338 concentrations in SPM with the urbanization gradient (see section 3.1, Fig. S1). Accordingly,  
339 correlations between Chry, Flt and BaA were tested between all the different types of samples  
340 (including SPM, flood sediments, atmospheric particles and RDS), and the potential sources  
341 of river particles (soils and urban runoff particles), along with the Seine River sediment

342 providing the signature of legacy contamination (Figure 4). As the range of PAH  
343 concentrations found in these samples was particularly large, the graph providing this  
344 comparison was plotted in log scale.

345 Overall, the correlations between Chry, Flt and BaA showed the occurrence of two trends, one  
346 composed of atmospheric particles and the second including the rest of the samples (Orge  
347 SPM, flood sediments, soil samples, runoff particles and Seine River sediments). Road  
348 deposited sediments appeared to be either included in the first (Figure 4a) or the second group  
349 depending on the PAH compounds considered (Figure 4b and 4c).

350 The similarities between soil and river samples (including sediments and SPM) highlighted by  
351 Chry, Flt and BaA correlations suggest an identical source and the conservation of those 4  
352 rings PAH during their transfer. For instance, the alignment observed for the Orge SPM and  
353 the Seine River sediments indicated the conservation of the correlation between current Orge  
354 SPM and past Seine River SPM, despite the significant differences in their PAH  
355 concentrations. Moreover, particles transported during the flood of June 2016 and deposited  
356 on banks during the overflow have been identified as old particles, long-term stored in the  
357 Orge catchment and remobilized by high water flow (Le Gall et al., 2018). Those floodplain  
358 sediments appeared to present a PAH signature similar to the Seine River sediments (Figure  
359 4). Therefore, those observations suggest that the current PAH contamination in the Orge  
360 River may reflect the global PAH accumulation over the catchment during more than a  
361 century of industrial activities (Lorgeoux et al., 2016; Pacyna et al., 2003). The signatures of  
362 runoff particles were also aligned with those of river particles and soil samples (Figure 4),  
363 although not with that of atmospheric particles. Those results tend to exclude atmospheric  
364 deposition as providing the major PAH primary source for runoff particles suggesting PAH  
365 released on urban surfaces as the main supply of PAH during runoff (Blanchard et al., 2001).  
366 In addition, the similarity between older sediments signature and those of current runoff also



367 supports the hypothesis of a long-term persistence of PAH in the river basin, characterized by  
368 the widespread and extensive contamination of soil samples, current Orge River SPM, and  
369 urban runoff particles as demonstrated by their PAH signature identical to that of legacy  
370 contamination (i.e. Seine River sediments).

371 The conservation of PAH signature over time and during the transfer of particles between the  
372 soils and the river observed here could be partly explained by a stabilization process occurring  
373 in soils during their aging, known to be responsible for the persistence of PAH in the  
374 environment (Biache et al., 2011), associated with their low degradation in the river.  
375 Depending on the soil characteristics (structure, organic matter content, microorganisms, etc.),  
376 PAH could be sequestered and stabilized in the soil reducing their availability (Cébron et al.,  
377 2013; Chung and Alexander, 2002), which could be explained by their strong sorption onto  
378 organic particles (Ghosh et al., 2003; Yang et al., 2008). Once stabilized in soil particles, the  
379 PAH might be less sensitive to degradation during erosion processes, explaining the similar  
380 signature found in both river and soil particles. In the river, oxidation processes may also  
381 affect PAH depending on the water composition (Miller and Zepp, 1979; Xia et al., 2009),  
382 physico-chemical conditions and microbial activity (Quantin et al., 2005). Nonetheless,  
383 studies showed that natural oxidation in water might be less important than expected based on  
384 the results of laboratory experiments because of the occurrence of multiple external factors  
385 such as variations in organic matter type and amount, microbial competition... (Fasnacht and  
386 Blough, 2002; Ge et al., 2016), reducing PAH degradation in rivers. Finally, the conservation  
387 of the PAH signature may also be explained by the similar degradation of the molecules in  
388 soils and sediments leading to a homogeneous signature of the contamination at the scale of  
389 the critical zone.

390 In contrast to river sediment and soil signatures, atmospheric particles showed a different  
391 pattern, with the occurrence of very variable signatures differing from those in river, soil and

392 runoff samples (Figure 4). This discrepancy suggests that the direct atmospheric  
393 contamination does not provide a major source of PAH for river particles, soil particles and  
394 urban runoff particles in the Orge River catchment, suggesting the dominance of the legacy  
395 contamination. Moreover, the atmospheric contamination was shown to be mainly related to  
396 the current PAH production in the atmosphere, such as vehicular emissions (Keyte et al.,  
397 2016; Oda et al., 2001) or household heating (Motelay-Massei et al., 2007) which could  
398 explain the variability of atmospheric particle signatures. In addition, 4 rings signatures of  
399 atmospheric particles might be modified by the occurrence of processes such as photo-  
400 oxidation or chemical oxidation in the atmosphere (Suess, 1976). For instance, the presence of  
401 reactive molecules ( $O_2$ ,  $NO_x$ ,  $SO_2$ ) may lead to a degradation of PAH (Finlayson-Pitts, 1997;  
402 Nikolaou et al., 1984). Multiple factors may also influence PAH degradation in the  
403 atmosphere such as the particle composition, especially the presence of soot particles  
404 suggested to protect PAH from photo-degradation (Zelenyuk et al., 2012), or the humidity  
405 level and the sunlight intensity (Ringuet et al., 2012). This susceptibility of PAH bound to  
406 atmospheric particles to various degradation processes combined with the potential source  
407 variability may explain the very scattered pattern of the atmospheric sample signatures  
408 compared to the stable pattern found in river sediment and soil samples.

409 Finally, RDS signatures showed a depletion in the BaA content (Figure 4b and c, and Figure  
410 3b), differentiating them from those urban runoff particles collected directly in separate storm  
411 sewers in Sucy. This depletion of BaA in RDS may be related to the higher sensitivity of BaA  
412 to changes in environmental conditions (temperature, availability of reactive compounds)  
413 compared to Chry and Flt and its faster degradation rate (Beyer et al., 2003; Butler and  
414 Crossley, 1981). As runoff and erosion are known to be particle-size selective, stormflow may  
415 have led to the preferential deposition of coarser particles on the road in Viry (i.e. RDS)  
416 whereas smaller particles ( $<100 \mu m$ ) have been washed away by rainfall (Andral et al., 1999;

417 Owens et al., 2011). These particles were then likely highly exposed to photo-degradation,  
418 which may explain the specific decrease in BaA concentrations in RDS collected on the road,  
419 further illustrating the great caution required when using BaA as a potential source indicator.

420 The relative conservation of particulate-bound Chr and Flt between soils, urban runoff  
421 particles, and river sediment suggests the potential of the Chr - Flt correlation to trace the  
422 sources of PAH contamination in the study area. Accordingly, this correlation was tested  
423 comparing the values found in the Orge River SPM collected at the different monitoring sites,  
424 with those of the potential sources and including soil samples, RDS and urban runoff particles  
425 (Figure 5). The correlation between Chr and Flt reflects the increasing PAH input in  
426 downstream direction and identifies RDS and urban runoff particles as the potential ultimate  
427 sources of particulate PAH contamination to SPM provided by urban areas.

428

#### 429 3.4. Radionuclide model to investigate PAH sources from urban areas

430 The estimated PAH contents in theoretical urban particles (TUP) were finally compared to  
431 those PAH concentrations found in RDS and runoff particles (Figure 6).

432 The modelled concentrations of PAH in TUP appeared to be similar to those of both RDS and  
433 runoff particles collected from storm sewers (Figure 6). This observation confirmed the  
434 conclusion derived from PAH correlations (Figure 5) that those latter particles as provide the  
435 major source of PAH transferred to the river from urban surfaces. Therefore, the combination  
436 of sediment fingerprinting approach (i.e. radionuclides) with PAH signatures was shown to  
437 provide consistent results and underlined urban runoff as the main source of PAH transiting in  
438 the Orge catchment.

439 The model results also indicated that PAH concentrations in TUP were more similar to those  
440 found in urban runoff particles from storm sewers compared to RDS (Figure 6). This suggests

441 that urban runoff particles collected from these sewers provide a better surrogate of the  
442 ultimate source of contaminated urban particles supplied to the river. This further confirms  
443 that the PAH composition of RDS might have been affected during their storage on the road  
444 and might also be influenced by the sampling method. The depletion in BaA concentrations in  
445 RDS supports the hypothesis of degradation processes, especially photo-degradation  
446 occurring during RDS storage on the road (Marquès et al., 2017; Xu et al., 2013). In addition  
447 to degradation processes, particle size sorting might also explain the lower PAH content  
448 found in RDS, as the finest particles enriched in PAH might have been directly supplied to the  
449 river by runoff (Aryal et al., 2005), while the coarser particles may have deposited on the  
450 road, explaining their lower PAH content. These differences should therefore be considered in  
451 future studies considering RDS as potential sources of contaminants in the rivers.

452 In the current research, fallout radionuclides were used to identify and predict the contribution  
453 of contrasted PAH sources in the Orge River catchment. However, these results should be  
454 interpreted with caution, given the potentially high reactivity of PAH molecules, and their  
455 variations depending on their sources and the environmental conditions prevailing in the study  
456 site. The transfer time of particles from urban surfaces to the river appears to be crucial, as it  
457 may affect to a large extent the PAH degradation rate. In the Orge River system, the fast  
458 transfer of particles once they have been supplied to the river (Froger et al., 2018) likely  
459 reduces the potential degradation of particulate PAHs in the river because of the absence of  
460 sediment storage in the channel in downstream sections of the river. This specific context  
461 likely explains the good match observed between the modelled signature of TUP and that of  
462 urban runoff particles collected in storm sewers. However, these results may likely not be  
463 directly extrapolated to other potential study sites, as the concentration of several PAH may  
464 decrease with increasing storage time of sediment in the river channel. Furthermore,  
465 additional exposition to PAH sources like vehicle exhaust fumes may explain the higher

466 contamination levels observed in particles stored on urban surfaces (Bomboi and Hernández,  
467 1991; Markiewicz et al., 2017). Moreover, the duration and the intensity of precipitation must  
468 also be considered when modeling the contamination behavior, as PAH concentrations in  
469 urban runoff tend to increase during storms (Blanchard et al., 2001). Nevertheless, the model  
470 based on radionuclide measurements to calculate theoretical PAH profiles of urban particles  
471 provided promising results: similar approaches could be used as a potential useful tool for  
472 characterizing contaminant dynamics and identifying their carrying phases.

473

#### 474 **4. Conclusions**

475 The current research demonstrated first the persistence of PAH legacy contamination in the  
476 catchment and the conservation of those compounds in the soil-river continuum, as PAH  
477 diagnostic ratio and PAH correlations showed identical signatures for current Orge River  
478 SPM, Seine River basin soils and historical sediments from the Seine River. Atmospheric  
479 particles appeared to present another signature indicating a different PAH source and pattern  
480 for those samples. Finally, the combination of PAH signature with sediment fingerprinting  
481 approach using radionuclides to model PAH concentrations of particles transferred to the river  
482 from urban surfaces gave promising results, pointing runoff particles as the main PAH source  
483 in urban area. This model also underlined discrepancies between road deposited sediments  
484 collected on the road and runoff particles collected from stormsewers showing the need to  
485 consider these potential differences when assessing PAH sources in urban catchment.

486

#### 487 **Acknowledgements**

488 This research was financially supported by Paris-Sud University (PhD grant), the "Initiative  
489 de Recherche Stratégique" ACE-ICSEN funded by the University Paris-Saclay and the Seine  
490 River research program PIREN-Seine

## References

- Alam, M.S., Delgado-Saborit, J.M., Stark, C., Harrison, R.M., 2013. Using atmospheric measurements of PAH and quinone compounds at roadside and urban background sites to assess sources and reactivity. *Atmos. Environ.* 77, 24–35. <https://doi.org/10.1016/j.atmosenv.2013.04.068>
- Andral, M.C., Roger, S., Montréjaud-Vignoles, M., Herremans, L., 1999. Particle Size Distribution and Hydrodynamic Characteristics of Solid Matter Carried by Runoff from Motorways. *Water Environ. Res.* 71, 398–407. <https://doi.org/10.2175/106143097X122130>
- Anyanwu, I.N., Semple, K.T., 2015. Fate and behaviour of nitrogen-containing polycyclic aromatic hydrocarbons in soil. *Environ. Technol. Innov.* 3, 108–120. <https://doi.org/10.1016/j.eti.2015.02.006>
- Aryal, R.K., Furumai, H., Nakajima, F., Boller, M., 2005. Dynamic behavior of fractional suspended solids and particle-bound polycyclic aromatic hydrocarbons in highway runoff. *Water Res.* 39, 5126–5134. <https://doi.org/10.1016/j.watres.2005.09.045>
- Bertrand, O., Mondamert, L., Grosbois, C., Dhivert, E., Bourrain, X., Labanowski, J., Desmet, M., 2015. Storage and source of polycyclic aromatic hydrocarbons in sediments downstream of a major coal district in France. *Environ. Pollut.* 207, 329–340. <https://doi.org/10.1016/j.envpol.2015.09.028>
- Beyer, A., Wania, F., Gouin, T., Mackay, D., Matthies, M., 2003. Temperature Dependence of the Characteristic Travel Distance. *Environ. Sci. Technol.* 37, 766–771. <https://doi.org/10.1021/es025717w>
- Biache, C., Ghislain, T., Faure, P., Mansuy-Huault, L., 2011. Low temperature oxidation of a

- coking plant soil organic matter and its major constituents: An experimental approach to simulate a long term evolution. *J. Hazard. Mater.* 188, 221–230.  
<https://doi.org/10.1016/j.jhazmat.2011.01.102>
- Biache, C., Mansuy-Huault, L., Faure, P., 2014. Impact of oxidation and biodegradation on the most commonly used polycyclic aromatic hydrocarbon (PAH) diagnostic ratios: Implications for the source identifications. *J. Hazard. Mater.* 267, 31–39.  
<https://doi.org/10.1016/j.jhazmat.2013.12.036>
- Blanchard, M., Teil, M.-J., Ollivon, D., Garban, B., Chestérikoff, C., Chevreuil, M., 2001. Origin and distribution of polyaromatic hydrocarbons and polychlorobiphenyls in urban effluents to wastewater treatment plants of the paris area (FRANCE). *Water Res.* 35, 3679–3687. [https://doi.org/10.1016/S0043-1354\(01\)00078-1](https://doi.org/10.1016/S0043-1354(01)00078-1)
- Bomboi, M.T., Hernández, A., 1991. Hydrocarbons in urban runoff: Their contribution to the wastewaters. *Water Res.* 25, 557–565. [https://doi.org/10.1016/0043-1354\(91\)90128-D](https://doi.org/10.1016/0043-1354(91)90128-D)
- Bressy, A., Gromaire, M.-C., Lorgeoux, C., Saad, M., Leroy, F., Chebbo, G., 2012. Towards the determination of an optimal scale for stormwater quality management: Micropollutants in a small residential catchment. *Water Res.* 46, 6799–6810.  
<https://doi.org/10.1016/j.watres.2011.12.017>
- Brown, J.N., Peake, B.M., 2006. Sources of heavy metals and polycyclic aromatic hydrocarbons in urban stormwater runoff. *Sci. Total Environ.* 359, 145–155.  
<https://doi.org/10.1016/j.scitotenv.2005.05.016>
- Budzinski, H., Jones, I., Bellocq, J., Piérard, C., Garrigues, P., 1997. Evaluation of sediment contamination by polycyclic aromatic hydrocarbons in the Gironde estuary. *Mar. Chem.* 58, 85–97. [https://doi.org/10.1016/S0304-4203\(97\)00028-5](https://doi.org/10.1016/S0304-4203(97)00028-5)



- Butler, J.D., Crossley, P., 1981. Reactivity of polycyclic aromatic hydrocarbons adsorbed on soot particles. *Atmos. Environ.* 15, 91–94. [https://doi.org/10.1016/0004-6981\(81\)90129-3](https://doi.org/10.1016/0004-6981(81)90129-3)
- Cébron, A., Faure, P., Lorgeoux, C., Ouvrard, S., Leyval, C., 2013. Experimental increase in availability of a PAH complex organic contamination from an aged contaminated soil: Consequences on biodegradation. *Environ. Pollut.* 177, 98–105. <https://doi.org/10.1016/j.envpol.2013.01.043>
- Chung, N., Alexander, M., 2002. Effect of soil properties on bioavailability and extractability of phenanthrene and atrazine sequestered in soil. *Chemosphere* 48, 109–115. [https://doi.org/10.1016/S0045-6535\(02\)00045-0](https://doi.org/10.1016/S0045-6535(02)00045-0)
- El-Mufleh, A., Béchet, B., Grasset, L., Rodier, C., Gaudin, A., Ruban, V., 2011. Distribution of PAH residues in humic and mineral fractions of sediments from stormwater infiltration basins. *J. Soils Sediments* 13, 531–542. <https://doi.org/10.1007/s11368-012-0586-x>
- Fasnacht, M.P., Blough, N. V., 2002. Aqueous Photodegradation of Polycyclic Aromatic Hydrocarbons. *Environ. Sci. Technol.* 36, 4364–4369. <https://doi.org/10.1021/es025603k>
- Fernandes, M.B., Sicre, M.-A., Boireau, A., Tronczynski, J., 1997. Polyaromatic hydrocarbon (PAH) distributions in the Seine River and its estuary. *Mar. Pollut. Bull.* 34, 857–867. [https://doi.org/10.1016/S0025-326X\(97\)00063-5](https://doi.org/10.1016/S0025-326X(97)00063-5)
- Fernández, P., Vilanova, R.M., Martínez, C., Appleby, P., Grimalt, J.O., 2000. The Historical Record of Atmospheric Pyrolytic Pollution over Europe Registered in the Sedimentary PAH from Remote Mountain Lakes. *Environ. Sci. Technol.* 34, 1906–1913. <https://doi.org/10.1021/es9912271>

- Finlayson-Pitts, B.J., 1997. Tropospheric Air Pollution: Ozone, Airborne Toxics, Polycyclic Aromatic Hydrocarbons, and Particles. *Science* (80-. ). 276, 1045–1051. <https://doi.org/10.1126/science.276.5315.1045>
- Froger, C., Ayrault, S., Evrard, O., Monvoisin, G., Bordier, L., Lefèvre, I., Quantin, C., 2018. Tracing the sources of suspended sediment and particle-bound trace metal elements in an urban catchment coupling elemental and isotopic geochemistry, and fallout radionuclides. *Environ. Sci. Pollut. Res.* 25, 28667–28681. <https://doi.org/10.1007/s11356-018-2892-3>
- Froger, C., Quantin, C., Gasperi, J., Caupos, E., Monvoisin, G., Evrard, O., Ayrault, S., 2019. Impact of urban pressure on the spatial and temporal dynamics of PAH fluxes in an urban tributary of the Seine River (France). *Chemosphere* 219, 1002–1013. <https://doi.org/10.1016/j.chemosphere.2018.12.088>
- Garban, B., Blanchoud, H., Motelay-Massei, A., Chevreuil, M., Ollivon, D., 2002. Atmospheric bulk deposition of PAHs onto France: trends from urban to remote sites. *Atmos. Environ.* 36, 5395–5403. [https://doi.org/10.1016/S1352-2310\(02\)00414-4](https://doi.org/10.1016/S1352-2310(02)00414-4)
- Gaspéri, J., Ayrault, S., Moreau-Guigon, E., Alliot, F., Labadie, P., Budzinski, H., Blanchard, M., Muresan, B., Caupos, E., Cladière, M., Gateuille, D., Tassin, B., Bordier, L., Teil, M.-J., Bourges, C., Desportes, A., Chevreuil, M., Moilleron, R., 2018. Contamination of soils by metals and organic micropollutants: case study of the Parisian conurbation. *Environ. Sci. Pollut. Res.* 25, 23559–23573. <https://doi.org/10.1007/s11356-016-8005-2>
- Gasperi, J., Sébastien, C., Ruban, V., Delamain, M., Percot, S., Wiest, L., Mirande, C., Caupos, E., Demare, D., Kessoo, M.D., Saad, M., Schwartz, J.J., Dubois, P., Fratta, C., Wolff, H., Moilleron, R., Chebbo, G., Cren, C., Millet, M., Barraud, S., Gromaire, M.-C., 2017. Contamination des eaux pluviales par les micropolluants : avancées du projet

INOGEV. Tech. Sci. Méthodes 51–70. <https://doi.org/10.1051/tsm/201778051>

Gateuille, D., Evrard, O., Lefevre, I., Moreau-Guigon, E., Alliot, F., Chevreuil, M., Mouchel, J.-M., 2014a. Mass balance and decontamination times of Polycyclic Aromatic Hydrocarbons in rural nested catchments of an early industrialized region (Seine River basin, France). *Sci. Total Environ.* 470–471, 608–617. <https://doi.org/10.1016/j.scitotenv.2013.10.009>

Gateuille, D., Evrard, O., Lefevre, I., Moreau-Guigon, E., Alliot, F., Chevreuil, M., Mouchel, J.M., 2014b. Combining measurements and modelling to quantify the contribution of atmospheric fallout, local industry and road traffic to PAH stocks in contrasting catchments. *Environ. Pollut.* 189, 152–160. <https://doi.org/10.1016/j.envpol.2014.02.029>

Ge, L., Na, G., Chen, C.-E., Li, J., Ju, M., Wang, Y., Li, K., Zhang, P., Yao, Z., 2016. Aqueous photochemical degradation of hydroxylated PAHs: Kinetics, pathways, and multivariate effects of main water constituents. *Sci. Total Environ.* 547, 166–172. <https://doi.org/10.1016/j.scitotenv.2015.12.143>

Ghosh, U., Zimmerman, J.R., Luthy, R.G., 2003. PCB and PAH Speciation among Particle Types in Contaminated Harbor Sediments and Effects on PAH Bioavailability. *Environ. Sci. Technol.* 37, 2209–2217. <https://doi.org/10.1021/es020833k>

Gocht, T., Ligouis, B., Hinderer, M., Grathwohl, P., 2007. ACCUMULATION OF POLYCYCLIC AROMATIC HYDROCARBONS IN RURAL SOILS BASED ON MASS BALANCES AT THE CATCHMENT SCALE. *Environ. Toxicol. Chem.* 26, 591. <https://doi.org/10.1897/06-287R.1>

Grimmer, G., 1985. PAH—Their contribution to the carcinogenicity of various emissions†. *Toxicol. Environ. Chem.* 10, 171–181. <https://doi.org/10.1080/02772248509357101>

- Harrison, R.M., Smith, D.J.T., Luhana, L., 1996. Source apportionment of atmospheric polycyclic aromatic hydrocarbons collected from an urban location in Birmingham, U.K. *Environ. Sci. Technol.* 30, 825–832 ST–Source apportionment of atmospheric.
- Haugland, T., Ottesen, R.T., Volden, T., 2008. Lead and polycyclic aromatic hydrocarbons (PAHs) in surface soil from day care centres in the city of Bergen, Norway. *Environ. Pollut.* 153, 266–272. <https://doi.org/10.1016/j.envpol.2007.08.028>
- Katsoyiannis, A., Breivik, K., 2014. Model-based evaluation of the use of polycyclic aromatic hydrocarbons molecular diagnostic ratios as a source identification tool. *Environ. Pollut.* 184, 488–494. <https://doi.org/10.1016/j.envpol.2013.09.028>
- Kavouras, I.G., Koutrakis, P., Tsapakis, M., Lagoudaki, E., Stephanou, E.G., Von Baer, D., Oyola, P., 2001. Source Apportionment of Urban Particulate Aliphatic and Polynuclear Aromatic Hydrocarbons (PAHs) Using Multivariate Methods. *Environ. Sci. Technol.* 35, 2288–2294. <https://doi.org/10.1021/es001540z>
- Keyte, I.J., Albinet, A., Harrison, R.M., Harrison, R.M., 2016. On-road traffic emissions of polycyclic aromatic hydrocarbons and their oxy- and nitro- derivative compounds measured in road tunnel environments. *Sci. Total Environ.* 566–567, 1131–1142. <https://doi.org/10.1016/j.scitotenv.2016.05.152>
- Le Gall, M., Ayrault, S., Evrard, O., Laceby, J.P., Gateuille, D., Lefèvre, I., Mouchel, J.-M., Meybeck, M., 2018. Investigating the metal contamination of sediment transported by the 2016 Seine River flood (Paris, France). *Environ. Pollut.* 240, 125–139. <https://doi.org/10.1016/j.envpol.2018.04.082>
- Le Pape, P., Ayrault, S., Quantin, C., 2012. Trace element behavior and partition versus urbanization gradient in an urban river (Orge River, France). *J. Hydrol.* 472–473, 99–110. <https://doi.org/10.1016/j.jhydrol.2012.09.042>

- Lorgeoux, C., Moilleron, R., Gasperi, J., Ayrault, S., Bonté, P., Lefèvre, I., Tassin, B., 2016. Temporal trends of persistent organic pollutants in dated sediment cores: Chemical fingerprinting of the anthropogenic impacts in the Seine River basin, Paris. *Sci. Total Environ.* 541, 1355–1363. <https://doi.org/10.1016/j.scitotenv.2015.09.147>
- Markiewicz, A., Björklund, K., Eriksson, E., Kalmykova, Y., Strömvall, A.-M., Siopi, A., 2017. Emissions of organic pollutants from traffic and roads: Priority pollutants selection and substance flow analysis. *Sci. Total Environ.* 580, 1162–1174. <https://doi.org/10.1016/j.scitotenv.2016.12.074>
- Marquès, M., Mari, M., Sierra, J., Nadal, M., Domingo, J.L., 2017. Solar radiation as a swift pathway for PAH photodegradation: A field study. *Sci. Total Environ.* 581–582, 530–540. <https://doi.org/10.1016/j.scitotenv.2016.12.161>
- Miller, G.C., Zepp, R.G., 1979. Effects of suspended sediments on photolysis rates of dissolved pollutants. *Water Res.* 13.
- Motelay-Massei, A., Ollivon, D., Garban, B., Chevreuil, M., 2003. Polycyclic aromatic hydrocarbons in bulk deposition at a suburban site: assessment by principal component analysis of the influence of meteorological parameters. *Atmos. Environ.* 37, 3135–3146. [https://doi.org/10.1016/S1352-2310\(03\)00218-8](https://doi.org/10.1016/S1352-2310(03)00218-8)
- Motelay-Massei, A., Ollivon, D., Garban, B., Tiphagne-Larcher, K., Chevreuil, M., 2007. Fluxes of polycyclic aromatic hydrocarbons in the Seine estuary, France: mass balance and role of atmospheric deposition. *Hydrobiologia* 588, 145–157. <https://doi.org/10.1007/s10750-007-0659-9>
- Motelay-Massei, A., Ollivon, D., Garban, B., Tiphagne-Larcher, K., Zimmerlin, I., Chevreuil, M., 2007. PAHs in the bulk atmospheric deposition of the Seine river basin: Source identification and apportionment by ratios, multivariate statistical techniques and

scanning electron microscopy. *Chemosphere* 67, 312–321.  
<https://doi.org/10.1016/j.chemosphere.2006.09.074>

Murakami, M., Nakajima, F., Furumai, H., 2005. Size- and density-distributions and sources of polycyclic aromatic hydrocarbons in urban road dust. *Chemosphere* 61, 783–791.  
<https://doi.org/10.1016/j.chemosphere.2005.04.003>

Nikolaou, K., Masclet, P., Mouvier, G., 1984. Sources and chemical reactivity of polynuclear aromatic hydrocarbons in the atmosphere — A critical review. *Sci. Total Environ.* 32, 103–132. [https://doi.org/10.1016/0048-9697\(84\)90125-6](https://doi.org/10.1016/0048-9697(84)90125-6)

Oda, J., Nomura, S., Yasuhara, A., Shibamoto, T., 2001. Mobile sources of atmospheric polycyclic aromatic hydrocarbons in a roadway tunnel. *Atmos. Environ.* 35, 4819–4827.  
[https://doi.org/10.1016/S1352-2310\(01\)00262-X](https://doi.org/10.1016/S1352-2310(01)00262-X)

Owens, P.N., Caley, K.A., Campbell, S., Koiter, A.J., Droppo, I.G., Taylor, K.G., 2011. Total and size-fractionated mass of road-deposited sediment in the city of Prince George, British Columbia, Canada: Implications for air and water quality in an urban environment. *J. Soils Sediments* 11, 1040–1051. <https://doi.org/10.1007/s11368-011-0383-y>

Pacyna, J.M., Breivik, K., Münch, J., Fudala, J., 2003. European atmospheric emissions of selected persistent organic pollutants, 1970–1995. *Atmos. Environ.* 37, 119–131.  
[https://doi.org/10.1016/S1352-2310\(03\)00240-1](https://doi.org/10.1016/S1352-2310(03)00240-1)

Pratt, C., Lottermoser, B.G., 2007. Mobilisation of traffic-derived trace metals from road corridors into coastal stream and estuarine sediments, Cairns, northern Australia. *Environ. Geol.* 52, 437–448. <https://doi.org/10.1007/s00254-006-0471-2>

Quantin, C., Joner, E.J., Portal, J.M., Berthelin, J., 2005. PAH dissipation in a contaminated

- river sediment under oxic and anoxic conditions. *Environ. Pollut.* 134, 315–322.  
<https://doi.org/10.1016/j.envpol.2004.07.022>
- Ravindra, K., Bencs, L., Wauters, E., De Hoog, J., Deutsch, F., Roekens, E., Bleux, N., Berghmans, P., Van Grieken, R., 2006. Seasonal and site-specific variation in vapour and aerosol phase PAHs over Flanders (Belgium) and their relation with anthropogenic activities. *Atmos. Environ.* 40, 771–785. <https://doi.org/10.1016/j.atmosenv.2005.10.011>
- Ravindra, K., Sokhi, R., Vangrieken, R., 2008. Atmospheric polycyclic aromatic hydrocarbons: Source attribution, emission factors and regulation. *Atmos. Environ.* 42, 2895–2921. <https://doi.org/10.1016/j.atmosenv.2007.12.010>
- Revitt, D.M., Lundy, L., Coulon, F., Fairley, M., 2014. The sources, impact and management of car park runoff pollution: A review. *J. Environ. Manage.* 146, 552–567.  
<https://doi.org/10.1016/j.jenvman.2014.05.041>
- Ringuet, J., Albinet, A., Leoz-Garziandia, E., Budzinski, H., Villenave, E., 2012. Diurnal/nocturnal concentrations and sources of particulate-bound PAHs, OPAHs and NPAHs at traffic and suburban sites in the region of Paris (France). *Sci. Total Environ.* 437, 297–305. <https://doi.org/10.1016/j.scitotenv.2012.07.072>
- Roger, S., Montrejaud-Vignoles, M., Andral, M., Herremans, L., Fortune, J., 1998. Mineral, physical and chemical analysis of the solid matter carried by motorway runoff water. *Water Res.* 32, 1119–1125. [https://doi.org/10.1016/S0043-1354\(97\)00262-5](https://doi.org/10.1016/S0043-1354(97)00262-5)
- Schifman, L.A., Boving, T.B., 2015. Spatial and seasonal atmospheric PAH deposition patterns and sources in Rhode Island. *Atmos. Environ.* 120, 253–261.  
<https://doi.org/10.1016/j.atmosenv.2015.08.056>
- Schwientek, M., Rügner, H., Beckingham, B., Kuch, B., Grathwohl, P., 2013. Integrated

- monitoring of particle associated transport of PAHs in contrasting catchments. *Environ. Pollut.* 172, 155–162. <https://doi.org/10.1016/j.envpol.2012.09.004>
- Soclo, H.H., Garrigues, P., Ewald, M., 2000. Origin of polycyclic aromatic hydrocarbons (PAHs) in coastal marine sediments: Case studies in Cotonou (Benin) and Aquitaine (France) Areas. *Mar. Pollut. Bull.* 40, 387–396. [https://doi.org/10.1016/S0025-326X\(99\)00200-3](https://doi.org/10.1016/S0025-326X(99)00200-3)
- Sofowote, U.M., Hung, H., Rastogi, A.K., Westgate, J.N., Deluca, P.F., Su, Y., McCarry, B.E., 2011. Assessing the long-range transport of PAH to a sub-Arctic site using positive matrix factorization and potential source contribution function. *Atmos. Environ.* 45, 967–976. <https://doi.org/10.1016/j.atmosenv.2010.11.005>
- Suess, M.J., 1976. The environmental load and cycle of polycyclic aromatic hydrocarbons. *Sci. Total Environ.* 6, 239–250. [https://doi.org/10.1016/0048-9697\(76\)90033-4](https://doi.org/10.1016/0048-9697(76)90033-4)
- Tobiszewski, M., Namieśnik, J., 2012. PAH diagnostic ratios for the identification of pollution emission sources. *Environ. Pollut.* 162, 110–119. <https://doi.org/10.1016/j.envpol.2011.10.025>
- Umbuzeiro, G.A., Franco, A., Martins, M.H., Kummrow, F., Carvalho, L., Schmeiser, H.H., Leykauf, J., Stiborova, M., Claxton, L.D., 2008. Mutagenicity and DNA adduct formation of PAH, nitro-PAH, and oxy-PAH fractions of atmospheric particulate matter from São Paulo, Brazil. *Mutat. Res. - Genet. Toxicol. Environ. Mutagen.* 652, 72–80. <https://doi.org/10.1016/j.mrgentox.2007.12.007>
- Xia, X., Li, G., Yang, Z., Chen, Y., Huang, G.H., 2009. Effects of fulvic acid concentration and origin on photodegradation of polycyclic aromatic hydrocarbons in aqueous solution: Importance of active oxygen. *Environ. Pollut.* 157, 1352–1359. <https://doi.org/10.1016/j.envpol.2008.11.039>



- Xu, C., Dong, D., Meng, X., Su, X., Zheng, X., Li, Y., 2013. Photolysis of polycyclic aromatic hydrocarbons on soil surfaces under UV irradiation. *J. Environ. Sci.* 25, 569–575. [https://doi.org/10.1016/S1001-0742\(12\)60083-7](https://doi.org/10.1016/S1001-0742(12)60083-7)
- Xu, J., Peng, X., Guo, C.S., Xu, J., Lin, H.X., Shi, G.L., Lv, J.P., Zhang, Y., Feng, Y.C., Tysklind, M., 2016. Sediment PAH source apportionment in the Liaohe River using the ME2 approach: A comparison to the PMF model. *Sci. Total Environ.* 553, 164–171. <https://doi.org/10.1016/j.scitotenv.2016.02.062>
- Yang, Y., Ligouis, B., Pies, C., Achten, C., Hofmann, T., 2008. Identification of carbonaceous geosorbents for PAHs by organic petrography in river floodplain soils. *Chemosphere* 71, 2158–2167. <https://doi.org/10.1016/j.chemosphere.2008.01.010>
- Yunker, M.B., Macdonald, R.W., Vingarzan, R., Mitchell, R.H., Goyette, D., Sylvestre, S., 2002. PAHs in the Fraser River basin: a critical appraisal of PAH ratios as indicators of PAH source and composition. *Org. Geochem.* 33, 489–515. [https://doi.org/10.1016/S0146-6380\(02\)00002-5](https://doi.org/10.1016/S0146-6380(02)00002-5)
- Zelenyuk, A., Imre, D., Beránek, J., Abramson, E., Wilson, J., Shrivastava, M., 2012. Synergy between Secondary Organic Aerosols and Long-Range Transport of Polycyclic Aromatic Hydrocarbons. *Environ. Sci. Technol.* 46, 12459–12466. <https://doi.org/10.1021/es302743z>
- Zhang, X.L., Tao, S., Liu, W.X., Yang, Y., Zuo, Q., Liu, S.Z., 2005. Source Diagnostics of Polycyclic Aromatic Hydrocarbons Based on Species Ratios: A Multimedia Approach. *Environ. Sci. Technol.* 39, 9109–9114. <https://doi.org/10.1021/es0513741>

## Figures and table captions:

*Figure 1 : The Orge River catchment - land uses pattern, location of river sampling site and rain water collector (A: location of Seine River basin in Northern France, B: location of the Orge River catchment in the Ile de France Region around Mega Paris City)*

*Figure 2 : Water discharge of the Orge and Yvette rivers at the sampling sites and timing of the sampling campaigns*

*Figure 3 : Molecular diagnostic ratios of river SPM, atmospheric particles, flood sediments and RDS from the Orge River catchment along with the corresponding signatures of soils (Gaspéri et al., 2018), runoff particles (Gasperi et al., 2017), and Seine River sediment (Lorgeoux et al., 2016)*

*Figure 4 : Correlation between fluoranthene, chrysene and benzo(a)anthracene in Log10 displaying Orge River SPM, atmospheric particles, RDS and flood sediments along with soil samples (Gaspéri et al., 2018), runoff particles (Gasperi et al., 2017), Seine River sediments (Lorgeoux et al., 2016)*

*Figure 5 : Chrysene and fluoranthene content for the Orge River SPM displayed by sampling site, compared to the values found in the potential sources, including RDS samples, soil samples (Gasperi et al., 2016) and urban runoff particles from the Sucy site (Gasperi et al., 2017)*

*Figure 6 : PAH concentrations of modeled theoretical urban particles along with those of (urban) runoff particles and road deposited sediments*

*Table 1 : Literature data compiled to trace PAH contamination in the Orge River catchment (see detailed dataset in Table S6)*

**Table 1**

	<b>Description</b>	<b>Significance</b>	<b>Reference</b>
<b>Soil samples</b>	Samples from the soil surface collected in 2009 – 2010 across the Seine River basin (n = 32)	Potential source of particulate-bound PAH	(Gaspéri et al., 2018)
<b>Runoff particles</b>	Particles collected in 2011 – 2012 from a storm sewer in Sucy catchment	Potential source of particulate-bound PAH from urban areas	(Gasperi et al., 2017)
<b>Seine River sediments</b>	Samples from a sediment core collected in the floodplain of the Seine River in 2008	Legacy contamination signature: 1950 – 1963: maximum PAH contamination 1970 – 2004: stabilized contamination	(Lorgeoux et al., 2016)

Figure 1  
[Click here to download high resolution image](#)

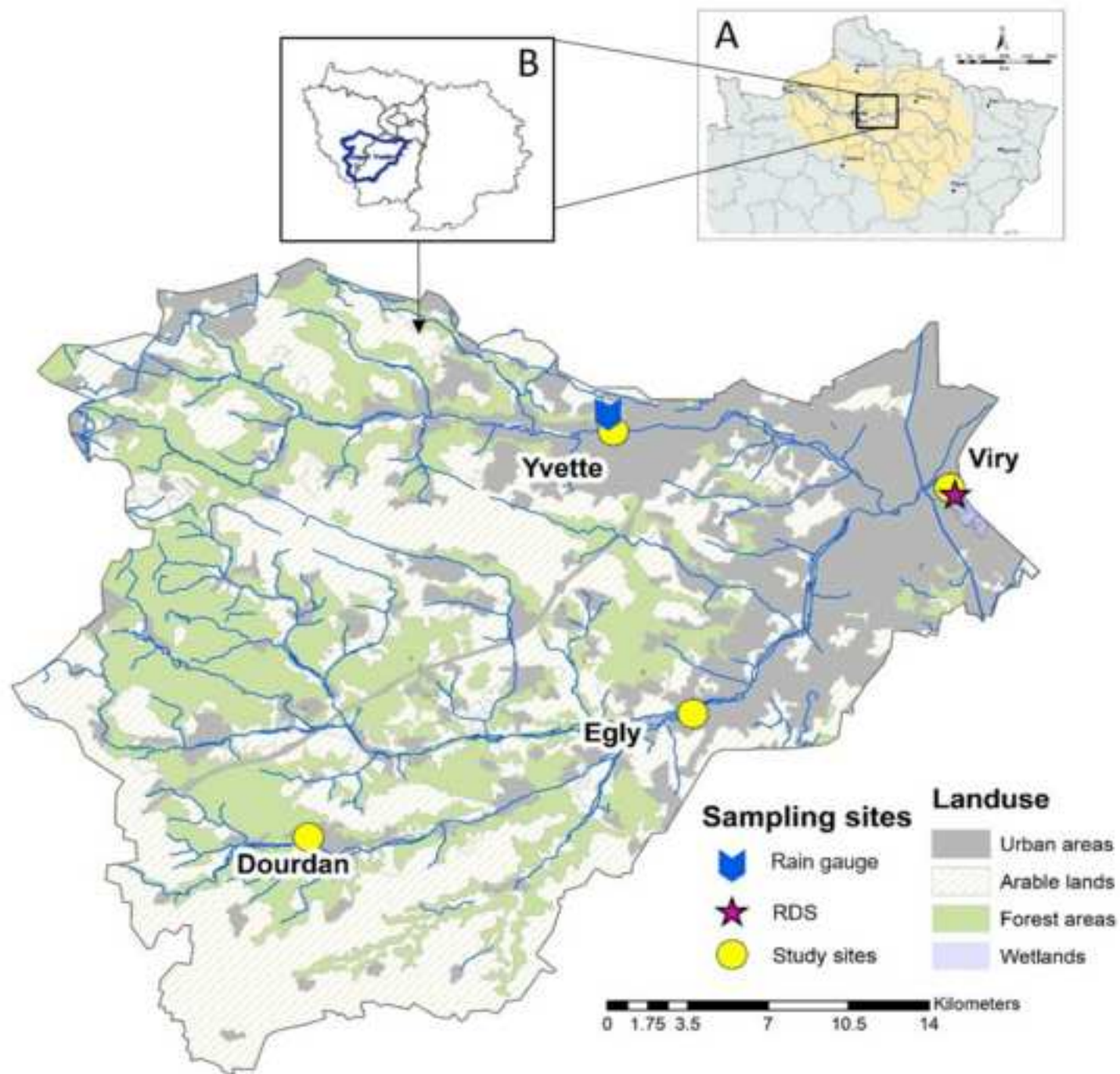


Figure 2  
[Click here to download high resolution image](#)

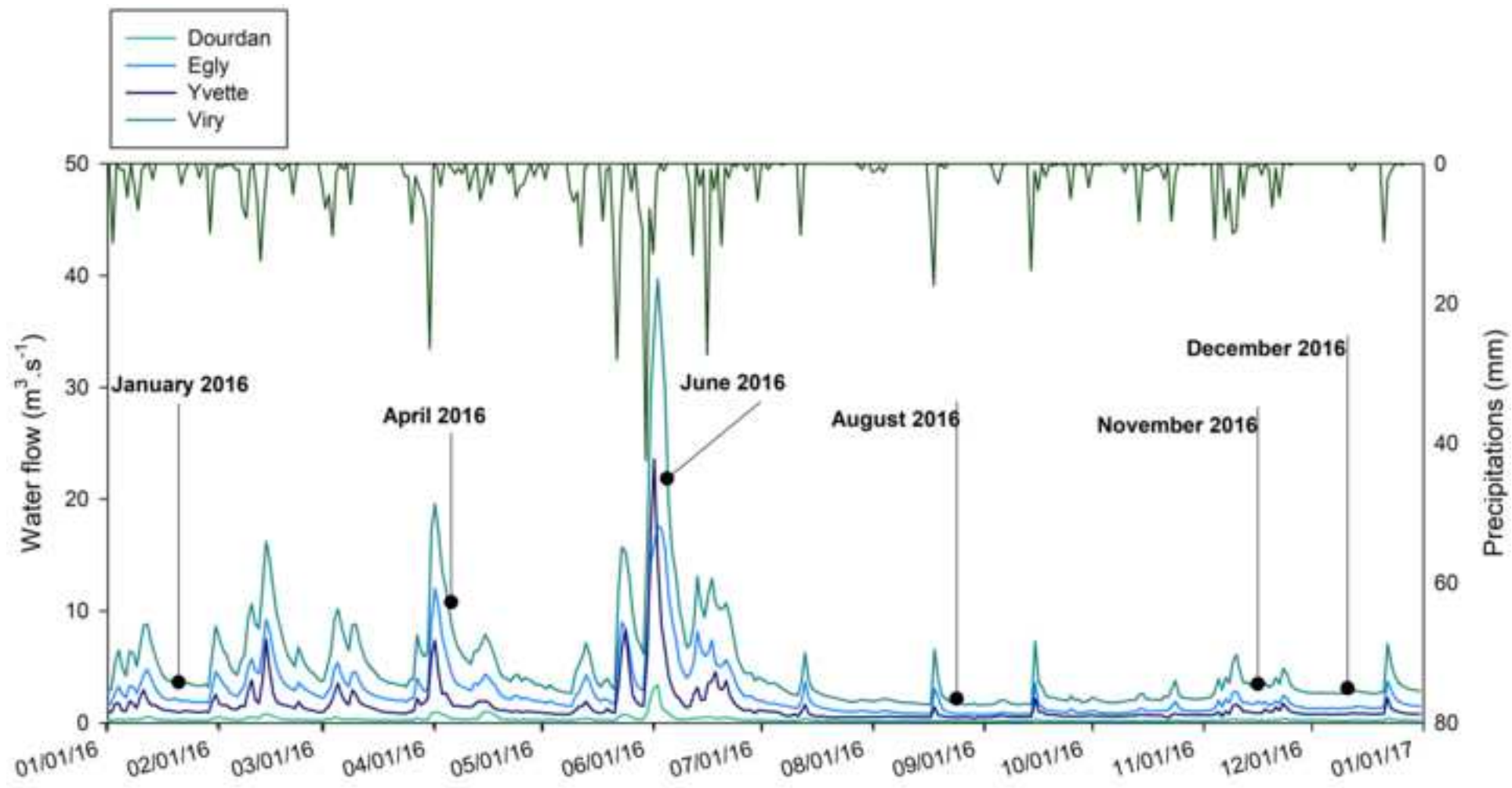


Figure 3  
[Click here to download high resolution image](#)

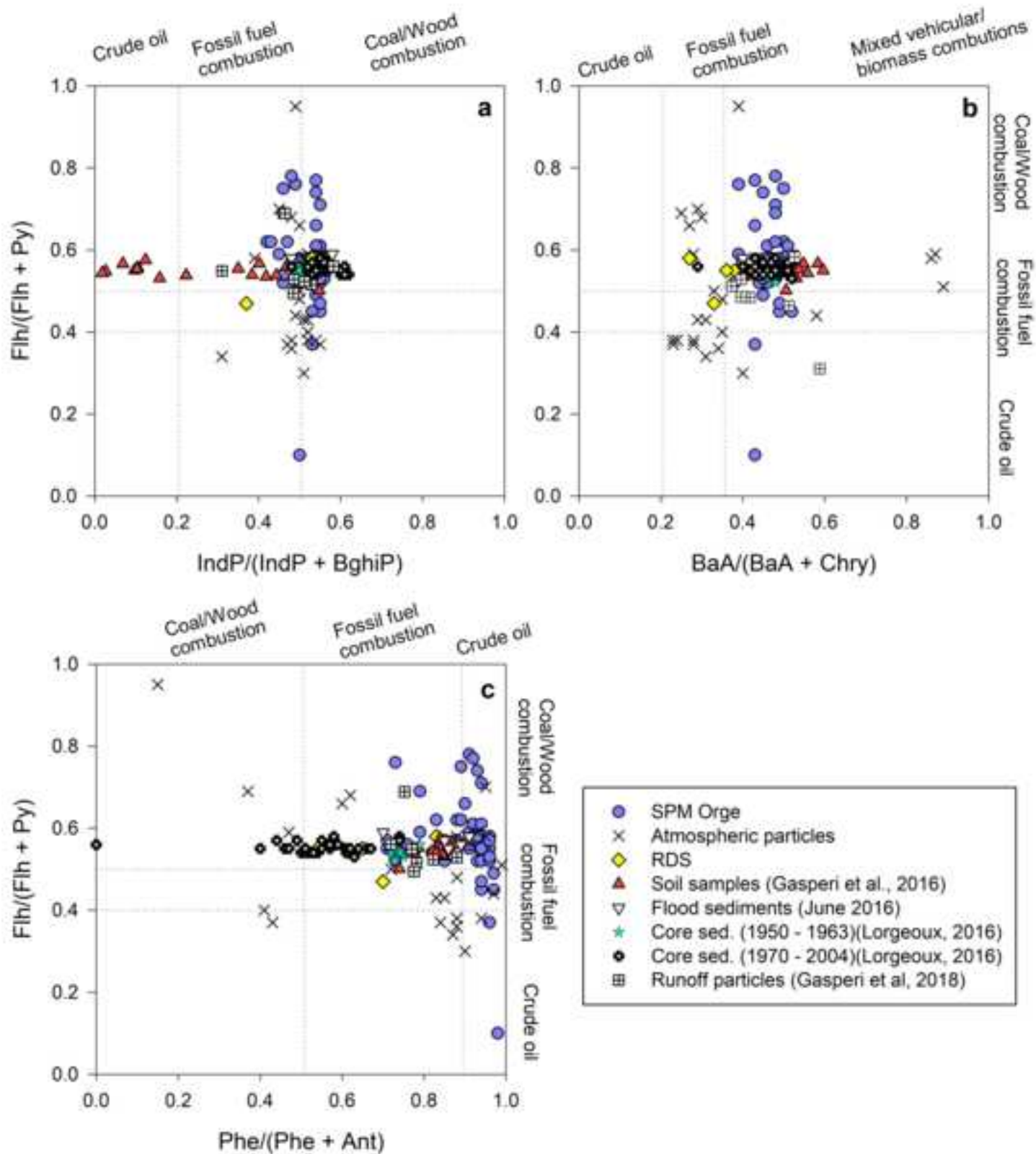


Figure 4  
[Click here to download high resolution image](#)

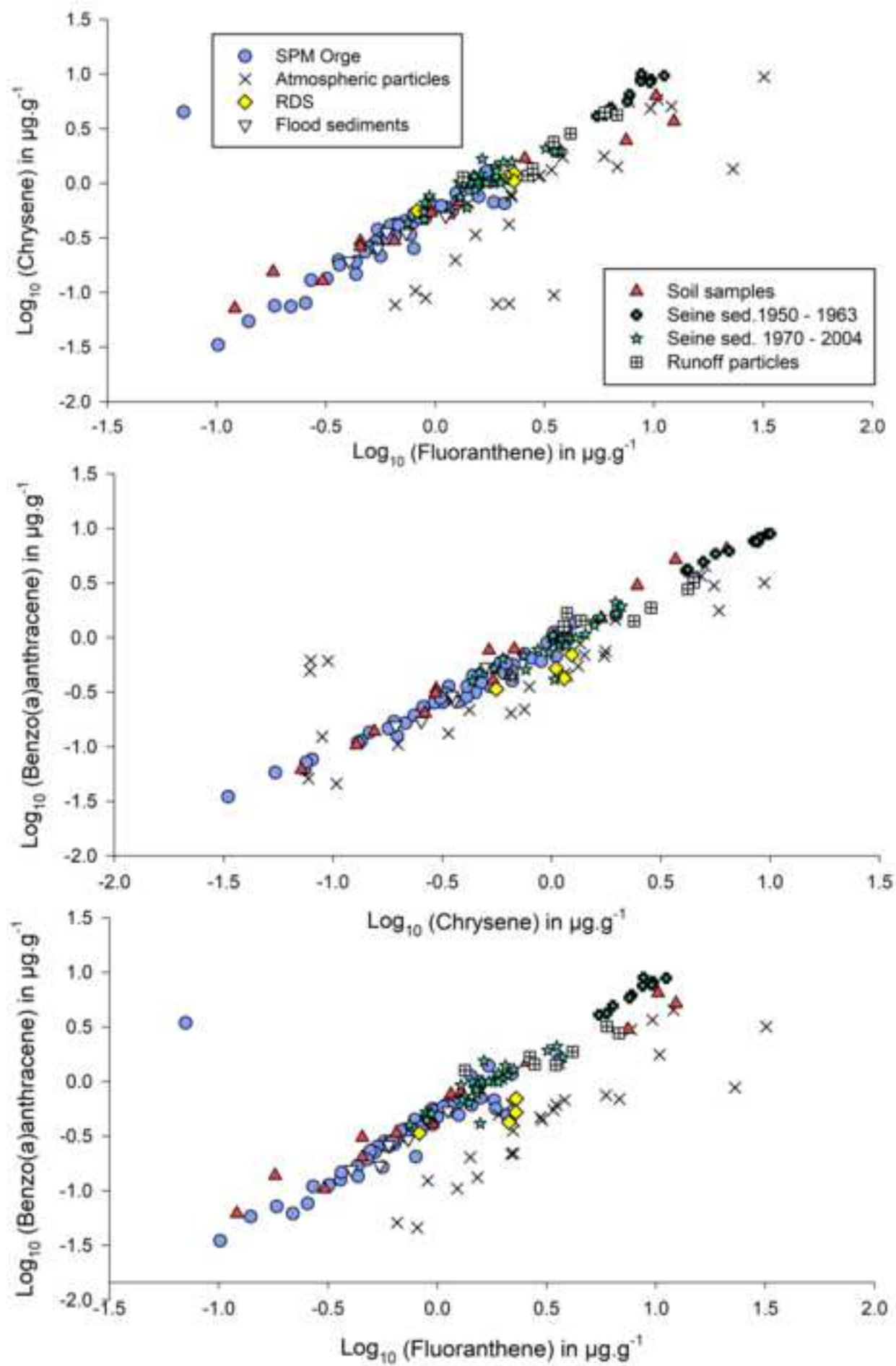


Figure 5  
[Click here to download high resolution image](#)

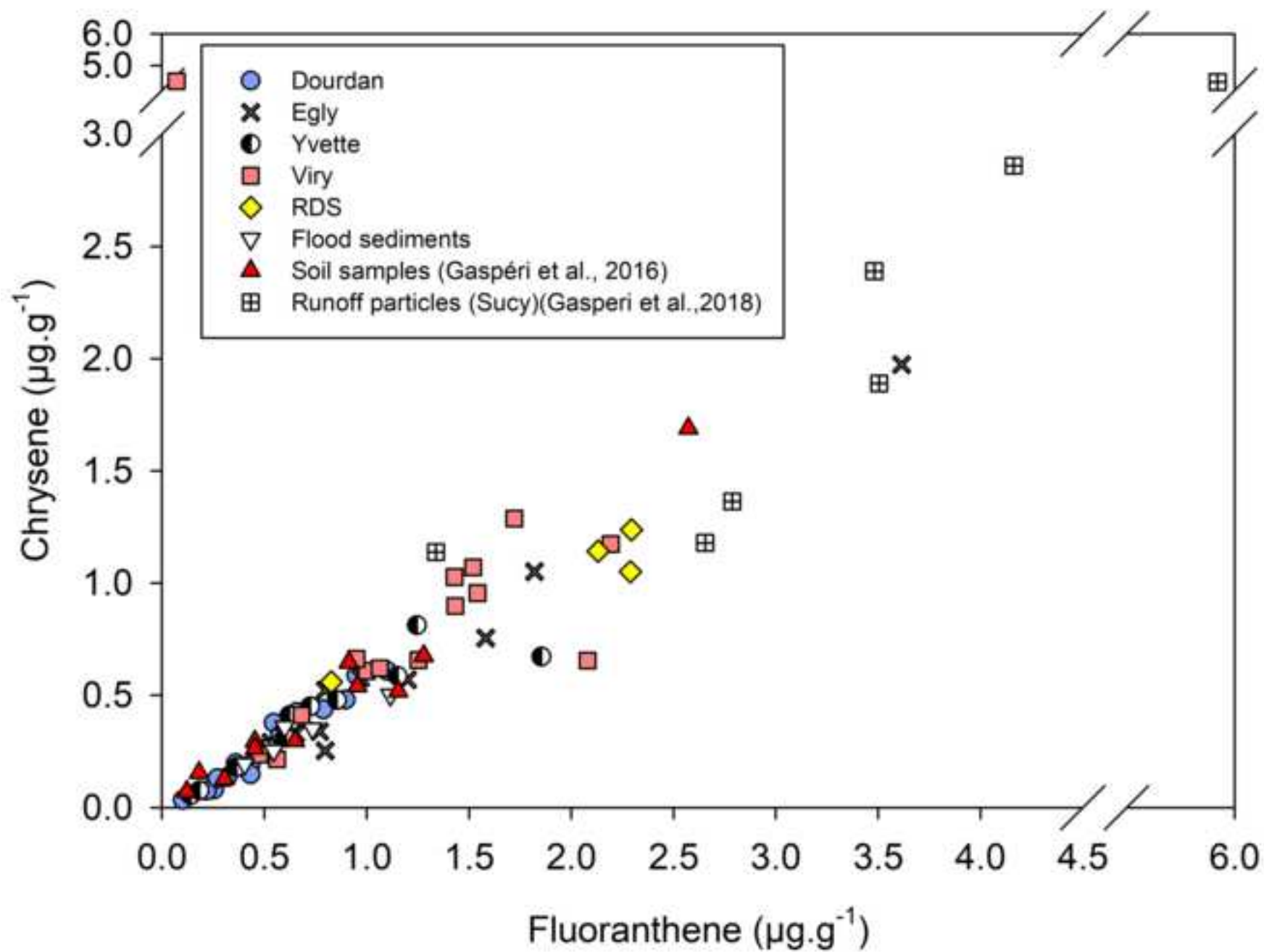
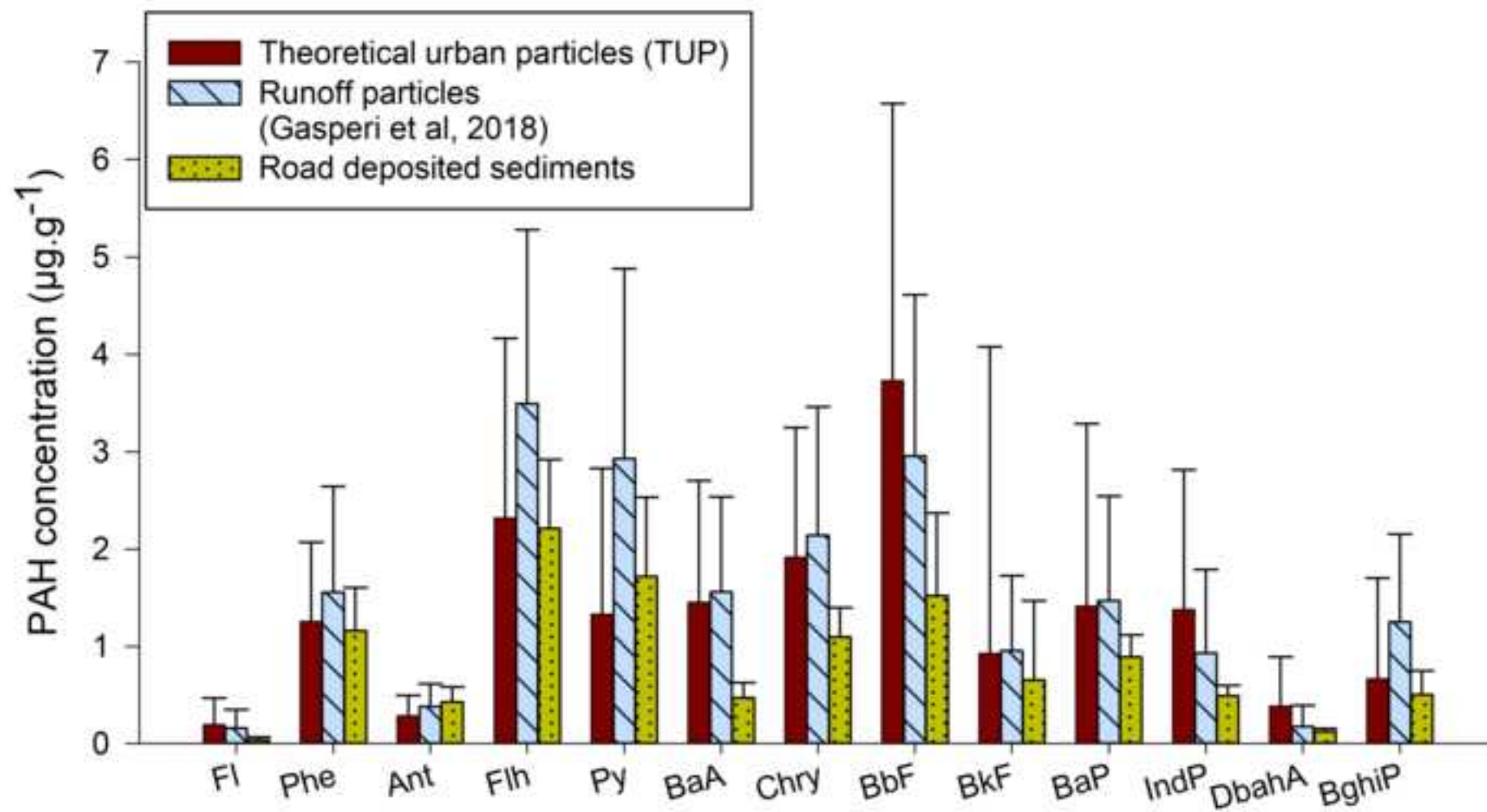




Figure 6  
[Click here to download high resolution image](#)



**Supplementary material for on-line publication only**

[Click here to download Supplementary material for on-line publication only: Supplementary\\_Froger\\_et\\_al\\_Tracing\\_PAH\\_source](#)